

5-10-2013

Utilization of an Anti-NNK Recombinant Antibody to Reduce the Harm Associated With Smokeless Tobacco

Heather L. Wanczyk

University of Connecticut - Storrs, Heather.Wanczyk@uconn.edu

Recommended Citation

Wanczyk, Heather L., "Utilization of an Anti-NNK Recombinant Antibody to Reduce the Harm Associated With Smokeless Tobacco" (2013). *Master's Theses*. 442.

https://opencommons.uconn.edu/gs_theses/442

This work is brought to you for free and open access by the University of Connecticut Graduate School at OpenCommons@UConn. It has been accepted for inclusion in Master's Theses by an authorized administrator of OpenCommons@UConn. For more information, please contact opencommons@uconn.edu.

**Utilization of an Anti-NNK Recombinant Antibody to Reduce the Harm
Associated With Smokeless Tobacco**

Heather Lauren Wanczyk

B.S., University of Connecticut, 2005

A Thesis

Submitted in Partial Fulfillment of the

Requirements for the Degree of

Master of Science

At the

University of Connecticut

2013

APPROVAL PAGE

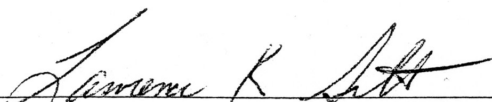
Masters of Science

Utilization of an Anti-NNK Recombinant Antibody to Reduce the Harm
Associated With Smokeless Tobacco

Presented by


Heather Lauren Wanczyk

Major Advisor



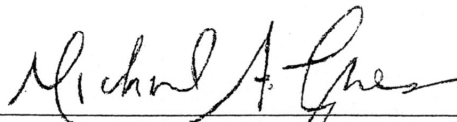
Lawrence Silbart

Associate Advisor



Paulo Verardi

Associate Advisor



Michael A. Lynes

University of Connecticut

2013

ACKNOWLEDGEMENTS

There are many individuals who I have to thank for all that I have accomplished in these past few years. First and foremost, I'd like to thank my major advisor Dr. Lawrence Silbart for having the faith to take on another Masters student. His guidance and support has allowed me to mature not only as a scientist, but also as a person. He granted me the ability to pursue my goals and excel in the field of Immunology, and for that I am eternally grateful. I'd also like to thank Debra Rood for her friendship and continued guidance throughout the years. I commend her for having the ability to make one feel at ease, even with the most intimidating of tasks. I'd also like to thank Sanjukta Majumder for being a good friend and always offering support when needed. I would also like to thank everyone who previously contributed to the following work including Tolga Barker, Debra Rood, John Zinckgraf, Daniel Zapata, Dr. Howell, Dr. Johnson, and Dr. Richardson. Without all these individuals, the present work would not have come as far as it has now. I also would like to thank my committee members, Dr. Lynes and Dr. Verardi, for their enthusiasm and support for the project. Last, but not least, I'd like to thank my husband John for his tireless love and encouragement for everything that I do. Without your continued support, this would not have been possible.

Table of Contents

Abstract	6
Introduction	7
1.1.1 Negative Health Effects of Chronic Tobacco Use	8
1.1.2 Tobacco Specific Nitrosamines	9
1.1.3 Metabolic Activation of TSNAs	10
1.1.4 Neurobiological Effects of Nicotine	12
1.1.5 Tobacco Harm Reduction	13
1.1.6 Monoclonal Antibodies	14
1.1.7 Recombinant Antibodies	14
Materials and Methods	19
2.1.1 Cloning and Characterization of F(ab)-generating single chain antibody	19
2.1.2 ELISA of F(ab)	20
2.1.3 Competitive ELISA of F(ab)	21
2.1.4 Cell Viability Assay	22
2.1.5 BrdU Proliferation Assay	22
2.1.6 Reconstruction of Plasmid Encoding Anti-NNK Recombinant Binding Fragment	24
2.1.7 Validation of Plasmid Vector Sequence	24
2.1.8 Coupled Transcription/Translation of Purified Plasmid	25

2.1.9 Purification of Final Protein Product	26
2.1.10 Protein Concentration	27
2.1.11 Re-Characterization of F(ab)-generating single chain antibody	28
2.1.12 Western Blot Analysis	28
2.1.13 Statistical Analysis	28
Results	29
3.1.1 PCR amplification of the V_H and V_L Immunoglobulin chains of the 7F Mab.	
3.1.2 The schematic map of BSA-DP-pFab-H	32
3.1.3 SDS-PAGE separation of purified Anti-NNK Binding Fragment	33
3.1.4 Western Blot Analysis	34
3.1.5 Competitive Inhibition of Anti-NNK Binding Fragment and 7F using free NNK	35
3.1.6 Final Plasmid Construct	36
3.1.7 DNA sequence of Optimized Anti-NNK Binding Fragment	37
3.1.8 Gel Analysis of DNA from Reconstructed Plasmid	39
3.1.9 SDS-PAGE of Anti-NNK Binding Fragment	40
Discussion	41
References	45

Abstract

Tobacco products, both combustible and smokeless, contain abundant amounts of toxic chemicals and carcinogens capable of causing extensive damage to the body. Tobacco specific nitrosamines, including 4-(methylnitrosoamino)-1-(3-pyridyl)-1-butanone (NNK) and N'-nitrosonornicotine (NNN), are among the most potent of these carcinogens and are capable of eliciting cellular transformations within the body after bioactivation by cytochrome P450 enzymes. In order to reduce the harm associated with smokeless tobacco, a recombinant anti-NNK antibody has been constructed from a hybridoma secreting a mouse monoclonal antibody specific for NNK.

In work performed previously, hybridomas were created by constructing a structurally-related benzoyl derivative to facilitate coupling to NNK-carrier proteins, which were then used to immunize BALB/C mice. Splenocytes from mice bearing NNK-specific antibodies were used for hybridoma production and the final product was isolated, characterized and found to secrete a high-affinity anti-NNK monoclonal antibody. In the current study, the heavy and light chain antibody F(ab) fragments were cloned, sequenced and inserted in tandem into an expression vector with an FMDV Furin 2A cleavage site between them. Expression in HEK 293 cells revealed a functional F(ab) with similar binding features to that of the parent hybridoma. This study lays the groundwork for synthesizing transgenic tobacco that expresses carcinogen-sequestration properties, thereby rendering it less harmful to consumers.

Introduction

1.1.1 Negative Health Effects of Chronic Tobacco Use

Tobacco use continues to be the main cause of lung cancer and cardiovascular disease worldwide and has been estimated to kill more than 6 million people each year [1,2]. Despite decades of continuous efforts to control the production and marketing of tobacco products, especially to youths, countless people still engage in this dangerous habit [3]. On average, it has been shown that cigarette smoking can reduce the lifespan of an individual by 13.5 years [4]. According to the World Health Organization, approximately one person dies every six seconds due to tobacco use, which accounts for one in ten adult deaths. The American Heart Association estimates that in 2004, tobacco use cost the United States \$193 billion dollars in healthcare and lost productivity.

Over the past decade, the number of people who smoke in the United States has declined by a small percentage. In 2011, the CDC estimated that there was about a 2-3% drop in the number of male and female smokers over a span of nine years (2000-2009). However, worldwide it has been estimated that there are 6 billion people who currently use some form of tobacco and out of this population, 80% live in low- and middle-income families [5]. These numbers are concerning considering that over 6,000 harmful chemicals and toxicants are consumed by an individual when a single cigarette is smoked. Around sixty of these compounds have been classified as known or suspected carcinogens and include polycyclic aromatic hydrocarbons, formaldehyde, benzene and tobacco specific nitrosamines (TSNAs) [6,7].

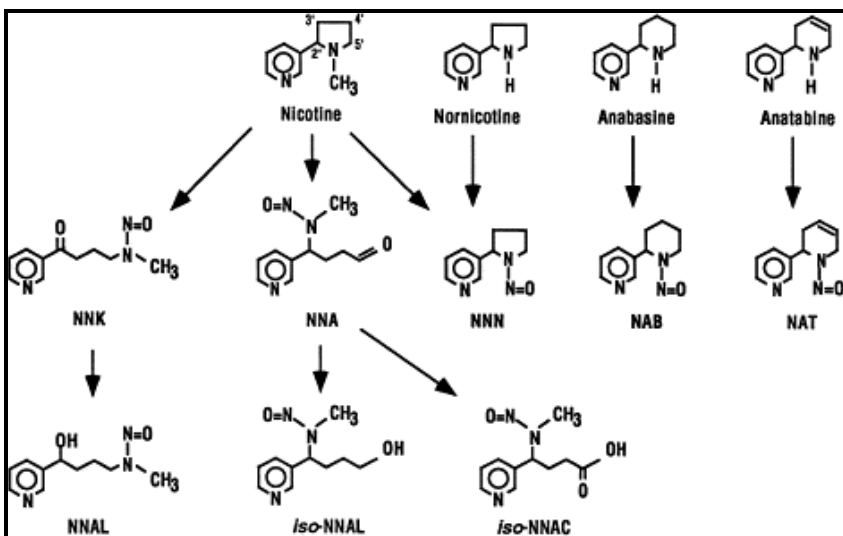
1.1.2 Tobacco Specific Nitrosamines

The most abundant and potent carcinogens found within cigarettes and smokeless tobacco products are tobacco specific nitrosamines, 4-(methylnitrosoamino)-1-(3-pyridyl)-1-butanone (**NNK**), 4-(Methylnitrosamino)-1-(3-pyridyl)-1-butanol (**NNAL**) and N'-nitrosonornicotine (**NNN**) [8,9]. Each of these nitrosamines contains a single N' nitroso moiety that is responsible for the carcinogenic nature of the compounds. NNK and NNN are classified as Group 1 human carcinogens by the International Agency for the Research on Cancer (IARC) and are formed from the nitrosation of the tobacco alkaloid nicotine [10]. This process involves the interaction of nicotine with a nitrate, nitrite or nitrogenous gas and occurs both during the curing and processing of tobacco and in the mammalian organism itself [11]. N'-nitrosonornicotine (NNN) is additionally formed by the demethylation of nicotine into nornicotine, which is then followed by nitrosation of the pyrrolidine nitrogen of nornicotine.

Minor secondary tobacco alkaloids such as anatabine and anabasine also participate in the formation of tobacco specific nitrosamines, but to a lesser extent than nicotine (**Figure 1.1**). Through reductive metabolism of NNK, NNAL is formed, which is another potent carcinogen [6]. It can be detected in the plasma and urine of cigarette users as well as people exposed to secondary smoke, making it an effective biomarker for the uptake of NNK. Higher urine NNAL has been proven to coincide with poorer physical health, restricted activity and dyspnea, which is an early predictor of lung cancer susceptibility [12,13].

Figure 1.1 Nitrosation of Tobacco Alkaloids [14]

Nitrosation of tertiary and secondary minor tobacco alkaloids results in the formation of Tobacco Specific Nitrosamines, some of the most potent chemicals contained within tobacco products.



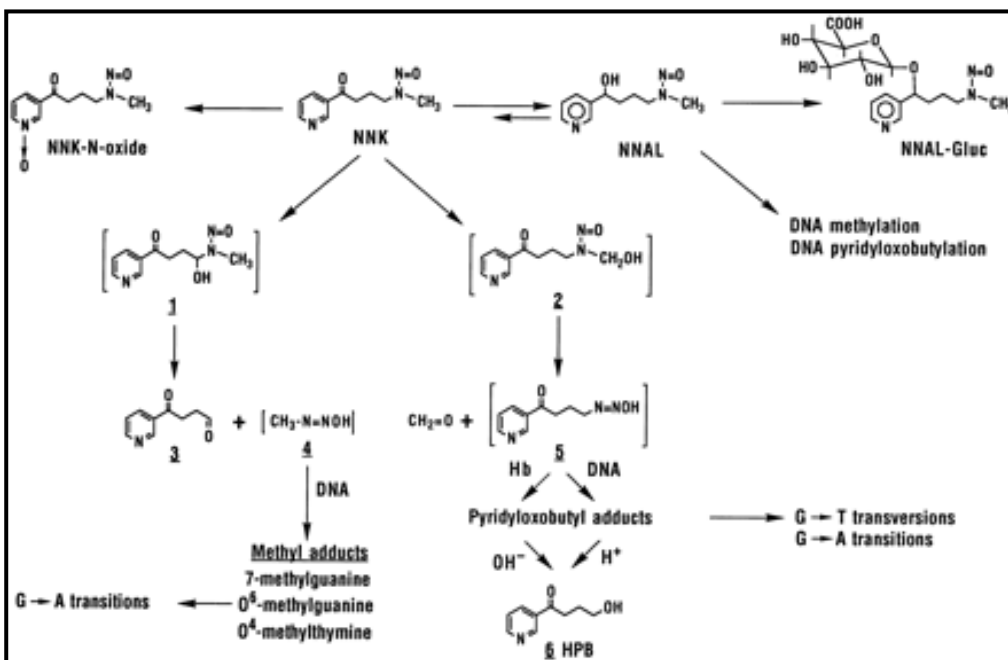
1.1.3 Metabolic Activation of TSNAs

In order to elicit cellular transformations within the body, the nitrosamines must be metabolically activated by cytochrome P450 enzymes such as CYP2A6 and CYP2A13, integral membrane proteins located within the endoplasmic reticulum of cells [15]. Although both enzymes play an important role in activation, CYP2A13 has been shown to activate NNK with a 61- to 214- fold greater catalytic efficiency than CYP2A6 [16-18]. Via hydroxylation pathways, NNK and NNN are metabolized into either methylating (7-methylguanine, O6-methylguanine) or pyridyloxobutylating (7-POB guanine, O2-POB thymine, O6-POB guanine) agents capable of forming DNA adducts,

which initiate mutations that contribute to tumor formation [8,6, 10, 19]. (**Figure 1.2**) In the current study, NNK is focused on exclusively due to the fact that it is the most potent carcinogen identified in smokeless and combustible tobacco products [20].

Figure 1.2 Metabolic Activation of NNK and DNA Adduct Formation [21]

Metabolic activation of NNK by Cytochrome P450 enzymes results in reactive intermediates that alkylate DNA. This leads to the formation of Pyridyloxobutyl or Methyl DNA adducts that are responsible for the initiation of tumor development.



In rodent studies, NNK has been shown to induce tumors in the lung, nasal and oral cavities, esophagus, liver and exocrine pancreas irrespective of the route of administration [8]. Further evidence for the carcinogenicity of NNK has been established in several in vitro studies whereby the nitrosamine induces the proliferation of normal

human lung epithelial cells, small cell lung cancer (SCLC) and non-small cell lung cancer (NSCLC) [15, 22,23, 24]. Proliferation can occur via alternative epigenetic mechanisms whereby the nitrosamine ligates with nicotinic acetylcholine receptors (nAChRs) located on the surface of epithelial cell membranes. These receptors are integral membrane proteins formed by the assembly of five trans-membrane subunits ($\alpha 3$, $\alpha 5$, $\alpha 7$, $\beta 4$) and exist in either homomeric or heteromeric forms [1]. **(Figure 1.3)** NNK binding causes a conformational change in the receptor, which induces a channel within the membrane to open, allowing for the influx of Na^+ and Ca^{+2} ions. Simultaneously, the efflux of K^+ ions occurs, resulting in membrane depolarization and the opening of voltage-gated Ca^{+2} channels. This influx of Ca^{+2} leads to enhanced activity in signaling pathways such as Protein Kinase C and A, Ras and PI3K, resulting in cell proliferation, angiogenesis, and apoptotic inhibition [25,26]. **Figure 1.4**

Figure 1.3- Nicotinic Acetylcholine Receptors [27]

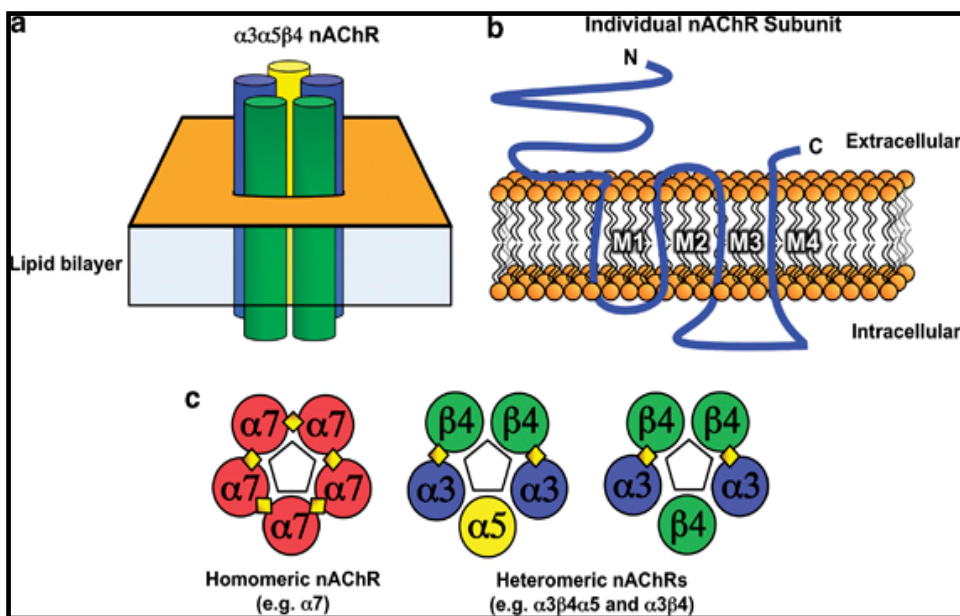
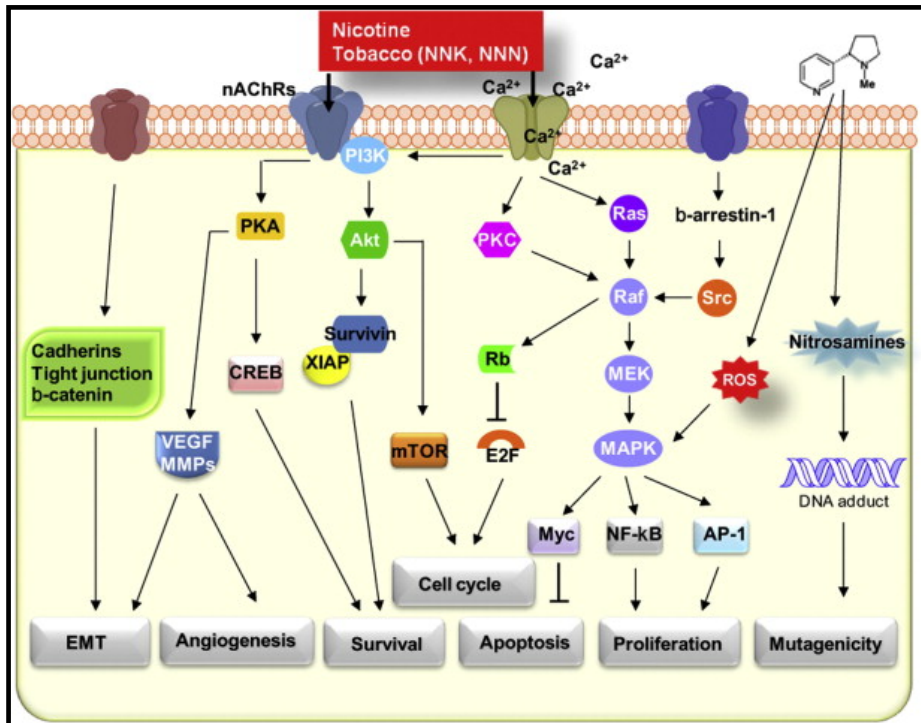


Figure 1.4- Signaling Pathways Activated by NNK

[<http://dx.doi.org/10.1016/j.jecm.2011.10.003>]



1.1.4 Neurobiological Effects of Nicotine

Considering all the facts and statistics pertaining to the detrimental effects of tobacco use, many individuals still succumb to this habit, and either refuse or are unable to quit. Out of the number of people that make the attempt, less than 5% are actually successful and only about one fifth of these individuals remain abstinent in the long run [28,1]. One of the reasons for this is that nicotine, the main component of tobacco, is extremely addictive. Once nicotine is inhaled, it rapidly passes through the blood brain barrier and binds to nicotinic acetylcholine receptors, leading to the activation of the “reward” circuitry of the brain and subsequent release of chemicals such as dopamine, glutamate and GABA. These chemicals elicit feelings of relaxation and euphoria. Long-

term usage of nicotine eventually results in neurobiological changes that lead to tolerance and addiction [29,30]. The effects of nicotine are so powerful and consuming that the overall experience is often compared to the effects elicited during use of hardcore drugs of abuse, i.e. cocaine and heroin [28].

1.1.5 Tobacco Harm Reduction

In the past few years, some public health officials have turned to tobacco harm reduction as an alternative means to reduce an individual's exposure to adverse chemicals and toxins within tobacco products. According to the American Council on Science and Health, tobacco harm reduction can be defined as “the substitution of far safer sources of nicotine by those smokers who are unable or unwilling to achieve nicotine/tobacco abstinence”. In countries such as Sweden, the use of snus, a moist powdered tobacco that is a variant of dry snuff, contains significantly lower levels of nitrosamines and has resulted in a marked decrease in cigarette smoking and the number of tobacco-related deaths among both men and women [31]. An epidemiological study done by Gartner in 2007 claimed that the health benefits from switching to low nitrosamine smokeless tobacco products are nearly as large as those from quitting tobacco use altogether [32]. In 2011, Rodu provided evidence, based on a comprehensive review of existing scientific and medical literature, that smokeless tobacco products on average have significantly less toxins and the risk of developing lung cancer is essentially abolished, making their use 90% safer than that of cigarettes [33]. In 2002, the Royal College of Physicians of London stated that the consumption of smokeless tobacco is 10-1,000 times less hazardous than smoking [33]. PREPs (non-combustible potential reduced exposure

products), have also been developed to reduce harmful tobacco exposure and include compressed tobacco tablets, nicotine water and patches, medicinal nicotine products and low nitrosamine cigarettes and smokeless tobacco products [34,35]. Although these products have been shown to be effective, many long-term tobacco users fail to quit because of the overpowering addictive properties of nicotine. Reduced exposure products that do not interfere with the free passage of nicotine within the brain would potentially save millions of lives worldwide.

1.1.6 Monoclonal Antibodies

In order to investigate alternative means for tobacco harm reduction, certain immunotherapies focused on mitigating the effects of debilitating drugs of abuse are currently in development. One such therapy involves the passive administration of poly- or monoclonal antibodies specific for drugs such as nicotine, heroin, cocaine and methamphetamine [36]. These antibodies are particularly effective due in part to their small molecular size, allowing for extensive tissue distribution and long elimination half-life following administration [37]. In 2009, Roiko et al passively immunized mice with a monoclonal antibody against nicotine and was able to successfully reduce the levels of the chemical within the brain [38]. Another study conducted by Norman et al in 2007 demonstrated that the intravenous administration of an anti-cocaine monoclonal antibody prior to the injection of cocaine was able to significantly decrease the levels of the substance within the brain of mice [39]. These are just a few of the many studies that highlight the potential for antibody-mediated interception as a therapeutic means to ameliorate or eliminate the toxicity associated with certain chemicals.

1.1.7 Recombinant Antibodies

The production of recombinant antibodies that express high affinity binding sites have become particularly attractive for immune-mediated sequestration of harmful toxins and chemicals. A way in which these sites can be created is through the use of 2A peptides derived from certain single-stranded RNA viruses. These peptides, which are usually around 18 amino acids long, mediate autonomous intra-ribosomal self-processing of multiple proteins from a single open reading frame [40]. In the current study, a 2A peptide derived from Foot and Mouth Disease Virus (FMDV) was used specifically for this purpose. The peptide originates from the viral family *Picornaviridae*, and functions by initiating “ribosomal skipping” at the glycine-proline peptide bond located within its highly conserved functional motif (D (V/I) EXNPGP) [41]. **(Figure 1.5)** This results in interruption of peptide bond formation at this location, leading to cleavage of the upstream protein. After this cleavage event occurs, translation of the downstream protein resumes **(Figure 1.6)**. All that remains of the 2A sequence on this protein is the proline. In order to remove the remainder of the 2A sequence from the upstream protein, a furin cleavage site is usually inserted just upstream of the sequence. Upon cellular processing, the remainder of the sequence is removed at this site and what remains are equal concentrations of both the downstream and upstream proteins.

In the work described herein, the 2A peptide derived from FMDV was used to create an anti-NNK recombinant binding site. This approach enabled the parent hybridoma to be expressed as a single chain antibody fragment. This antibody format is beneficial because its smaller structure facilitates ease of cloning into expression vectors, elicits minimal immunogenicity and is rapidly cleared from the circulation [31]. Following production,

the recombinant antibody, delivered by the appropriate vector or admixed with the product, may be used to passively protect the oral cavity prior to or during smokeless tobacco use. NNK bioactivation will be prevented once the high-affinity antibody binds to its target and the complex is predicted to be harmlessly eliminated through expectoration. According to a study conducted by Hecht et al (2007), daily exposure of NNK in smokeless tobacco users is ~6 µg, when an average of 2 grams tobacco is chewed. The study also found that the average concentration of NNK in expectorated saliva of 15 smokeless tobacco users was 3.2 nmol [42]. Based on these findings, tests will need to be conducted to determine the optimal molar concentration of binding fragment vs. NNK in saliva in order to elicit the desired protective response. After the appropriate concentrations have been determined, the safety and efficacy of this approach will be tested in animal models and humans.

Another consideration that must be taken into account is the complex environment in which the recombinant binding fragment will be introduced. The oral cavity contains many different cells responsible for maintaining homeostasis and initiating proteolytic degradation of food and foreign substances, some of which include lymphocytes, acinar cells, squamous epithelial cells and bacterial cells. In addition to this, saliva also contains many different electrolytes, anti-bacterial compounds and several proteases [43]. Tests will be necessary to determine the extent to which these components may affect antigen-antibody complex formation within the oral cavity.

A long-term goal of the current proposal is to produce transgenic tobacco that allows the free passage of nicotine from the product, but blocks the bioavailability of carcinogens like NNK by immuno-interception. The expression of recombinant

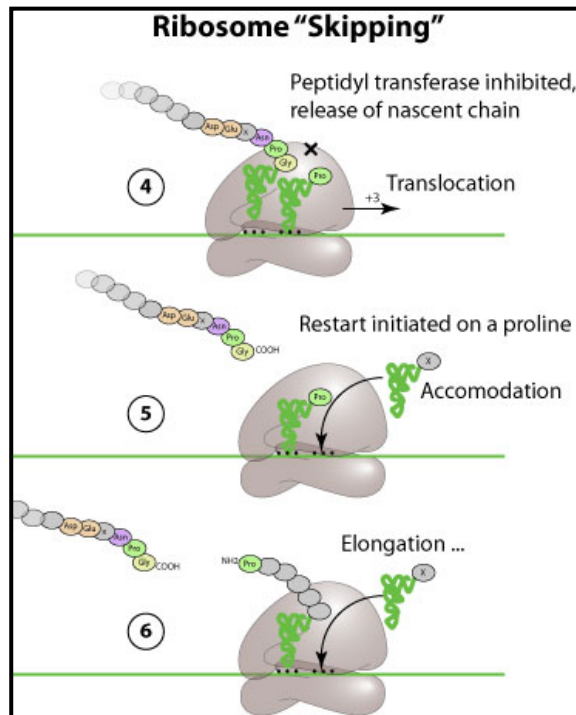
antibodies in tobacco has already proven to be technically feasible and will allow for the large-scale production of therapeutic antibodies at relatively low costs, making this approach particularly attractive to individuals seeking cost-effective tobacco harm reduction products.

Figure 1.5: Highly Conserved 2A Sequences [44]

Family	Example(s)	Abbr.	Sequences
			2A 'Cleavage' Site ↓
Picornaviridae	FMDV	F2A	VKQTLNFDLLKLAGDVESNPG P
	ERAV	E2A	QCTNYALLKLAGDVESNPG P
	PTV1	P2A	ATNFSLLKQAGDVEENPG P
Tetraviridae	TaV	T2A	EGRGSLLTCGDVEENPG P

Figure 1.6: Mechanism of Cleavage Event Initiated by Viral 2A Peptide

Ribosomal skipping is initiated by the viral 2A peptide through interruption of the peptide bond between the glycine and proline that are located within its highly conserved functional motif.



http://www.google.com/imgres?imgurl=http://education.expasy.org/images/Ribskip.jpg&imgrefurl=http://viralzone.expasy.org/all_by_protein/914.html

Materials and Methods

2.1.1 Cloning and Characterization of F(ab)-generating single chain antibody:

Four T-75 culture flasks containing 7F cells in HybriCare Media supplemented with MEM Sodium Pyruvate (100 mM), MEM Non-essential AA (10 mM), L-Glutamine (200 mM), 1× AB/AM and 20% heat inactivated FBS were sent to Creative Biolabs (Shirley, NY, USA) for amplification and sequencing. An intervening 2A motif derived from FMDV was cloned into the expression vector 7Fmab_pFab-HL via restriction enzymes EcoRI and NotI. The amplified V_H and V_L Immunoglobulin chains of the antibody flanked the peptide linker and a furin cleavage site was inserted just upstream of the 2A motif. The construct was transfected into HEK293 cells to allow for cleavage and subsequent expression of the recombinant binding fragment. Under denaturing conditions, an SDS-PAGE was performed according to [45] in order to verify cleavage and the appropriate molecular weight of the polyprotein. Next, a Western Blot was performed to test the protein's immunoreactivity to a Fab-specific antibody. The primary antibody used was an Anti-Mouse IgG (Fab-specific) conjugated to alkaline phosphatase (Sigma-Aldrich, St. Louis, MO, USA) and diluted 1:10,000 in PTA/BSA 0.1% buffer (0.05 M phosphate buffer saline (PBS) + tween 20 (Aldrich, Milwaukee, WI, USA) + 0.01% sodium azide (Fluka, Buchs Sg, Switzerland)), with 0.1% ovalbumin added to the buffer pH 7.4. A second Western Blot was performed using a 1:40,000 dilution of the Anti-Mouse IgG (Fab-specific) antibody in order to better visualize the Immunoglobulin chains.

2.1.2 ELISA of F(ab):

ELISA was performed to test the binding of the F(ab) to its target antigen (NNK). One 96-well plate was coated with 10 µg/mL NNKB-Ovalbumin and 10 µg/mL Ovalbumin. Each of the coating solutions were diluted in 0.05 M sodium carbonate buffer (Sigma-Aldrich Inc. St. Louis, MO, USA), pH 9.6. The plate was wrapped in two layers of Parafilm and incubated at room temperature (21 °C) overnight. The next morning, a 1:8 dilution of the protein was made in PTA/BSA 0.1% buffer. A 1:2500 dilution of 7F was also made up to test on the same plate in order to compare the binding efficacies of the complete IgG versus the anti-NNK binding fragment. After the solutions were mixed, the 96-well plate was washed five times with PTA/BSA 0.1% buffer using a Bio-Tek ELx405 Microplate Washer. The plate was then blotted dry on paper towels. Fifty microliters/well of each antibody was added to their corresponding locations within the plate. The plate was then placed at room temperature for overnight incubation. The following morning, the plate was washed three times in PTA/BSA 0.1% buffer and blotted dry as above. A 1:1,000 dilution of Polyvalent Anti-Mouse IgG, A, M antibody conjugated to Alkaline Phosphatase was made up for application to the wells containing the 7F antibody. A 1:10,000 dilution of anti-Mouse IgG (Fab-specific) antibody conjugated to Alkaline Phosphatase was made for application to the wells containing the F(ab). Fifty microliters of each solution was then added to the appropriate wells. After a two hour incubation at room temperature the plate was washed 3 times once again using PTA/BSA 0.1% buffer. Two 5 mg tablets of the phosphatase substrate PNPP (Sigma-Aldrich, Lot # 120N8201V, St. Louis, MO, USA) were diluted in 10 mL of 0.05 M sodium carbonate + 0.001 M magnesium chloride (Sigma-Aldrich Inc. St. Louis MO,

USA) pH 9.8 and 50 μ L of this mixture was added to each of the wells. Results were then read at 25, 50, and 100 min using a Bio-Tek uQuant Universal Microplate Spectrophotometer set at a wavelength of 405 nm (Biotek Instruments, Winooski, VT, USA).

2.1.3 Competitive ELISA of F(ab):

A competition ELISA using the F(ab) was performed with NNK as the soluble competitor. The monoclonal antibody 7F was used as a positive control. A stock solution of NNK was made at a concentration of 48.25 mM (10 mg/mL) in de-ionized water. This solution was then diluted to 966 μ M, 292 μ M, 88.0 μ M and 26.0 μ M. 125 μ L of each dilution of NNK was added to separate test tubes, which contained 125 μ L of either a 1:4 dilution of F(ab) or a 1:1250 dilution of 7F. The samples were then mixed and incubated at room temperature for 30 min in order to allow for appropriate competition to occur. 50 μ L of each test tube containing the samples were added to their corresponding wells. After a 2 hr incubation period, plates were washed three times as above. A 1:10,000 dilution of anti-Mouse IgG (Fab-specific) antibody conjugated to Alkaline Phosphatase was then applied to the F(ab)-containing wells and a 1:1,000 dilution of Anti-Mouse IgG, A, M antibody conjugated to Alkaline Phosphatase was applied to 7F-containing wells, each at a volume of 50 μ L/well. Plates were then washed as above followed by PNPP substrate addition. Results were read at 25, 50 and 100 min intervals with the Bio-tek spectrophotometer set at a wavelength of 405 nm.

2.1.4 Cell Viability Assay:

To test the ability of the F(ab) to block the harmful effects of NNK on susceptible cells, the lung adenocarcinoma cell line A549 was purchased from ATCC. Cells were grown in F-12K media supplemented with 10 % FBS and 1x Ab/Am. Media was changed every 2-3 days and cells were passaged when they reached 70-80% confluency. To determine cell viability after exposure to NNK, cells were transferred to an opaque 96-well plate at a density of 6×10^3 cells per well. After 24 hours in F-12K media supplemented with 10% FBS, media was switched to 0.05% FBS to remove any exogenous growth factors that would affect the interaction of NNK with the cells. A 10 mg/mL stock solution of NNK was diluted to 2,500 $\mu\text{g/mL}$, 250 $\mu\text{g/mL}$, 25 $\mu\text{g/mL}$, 2.5 $\mu\text{g/mL}$ and 0.25 $\mu\text{g/mL}$ in F-12K media containing 0.05% FBS. After another 24 hours, the NNK solutions were added at 100 $\mu\text{L/well}$ to the plate. Cell viability of the cells was determined 24 hours later by performing a Cell Titer Glo Assay. Results were read on a FluoStar Optima Luminometer from BMG Labtech (Cary, NC, USA) at 45 minutes post application of the Cell Titer Glo reagent per manufacturer's protocol.

2.1.5 BrdU Proliferation Assay:

A BrdU Proliferation Assay was performed in order to determine the effect of NNK on transformed lung epithelial cells in vitro. NCI-H441 cells were purchased from ATCC and grown in RPMI-1640 media supplemented with 10% FBS and 1x Ab/Am. Media was changed every 4-5 days and cells were passaged when they reached 70-80% confluency. To determine cell proliferation after exposure to varying concentrations of NNK, freshly trypsinized cells dilute either 1:10 or 1:15 in fresh RPMI-1640 media

supplemented with 10% FBS and 1x Ab/Am, were seeded in 96-well plates at a density of 5×10^3 /well. Plates were then covered and placed in 37°C, 5% CO₂ for 24 hrs. The following day, cells were serum-starved to remove any exogenous growth factors by replacing media with 0.12% FBS. Cells were then placed in 37°C, 5% CO₂ for an additional 24 hrs. After cells reached 30% confluency, 10-fold serial dilutions of NNK (10mg/mL) mixed with RPMI-1640 media supplemented with 0.12% FBS were added to corresponding wells (0.483 µM, 4.83 µM, 48.3 µM, 483 µM, and 4,830 µM NNK). Control wells contained cells mixed with RPMI-1640 media supplemented with 0.12% FBS and no NNK. Plates were placed in 37°C, 5% CO₂ for a 2 hour incubation period.

20 µL/well of BrdU reagent was then added to the appropriate wells and cells were incubated for a total of 24hrs. Cells were then fixed and denatured according to the manufacturer's protocol. Wash buffer was added to the plates for a total of three times, aspirated after the final wash and blotted dry on paper towels. 100 µL/well of anti-BrdU monoclonal antibody was then added to the appropriate wells and incubated at room temperature for 1 hour. Plates were washed as above and blotted dry on paper towels. Goat anti-Mouse IgG, Peroxidase Conjugate was added at 100 µL/well and incubated at room temperature for a total of 30 min. Plates were once again washed 3 times and blotted dry on paper towels. 100 µL/well of TMB Peroxidase Substrate were added to corresponding wells and incubated at room temperature in the dark for 30 min. After the 30 min. incubation period, 100 µL/well of the acid Stop Solution was pipetted into the appropriate wells. Positive wells which corresponded to proliferating cells changed from blue to bright yellow. Results were read using a Bio-Tek uQuant Universal Microplate

Spectrophotometer set at a wavelength of 490 nm (Biotek Instruments, Winooski, VT, USA).

2.1.6 Reconstruction of Plasmid Encoding Anti-NNK Recombinant Binding

Fragment

Using the previously cloned antibody sequence, adjustments were made to the first plasmid vector (7F Fab) to improve overall binding affinity of the anti-NNK recombinant binding fragment. 7F V_L-C_L DNA was amplified from the 7F Fab vector using the primers U7fvl/Dck and ligated into pUC57 via *Pst*I/*Mfe*I, yielding the vector designated as **pUC57s-7FVLCL**. 7F V_H-CH1 DNA was then amplified from the 7F Fab vector using the primers U7fvh/Dch1 and ligated into pUC57-7FVLCL via *Sac*II/*Avr*II. The identity of the sequences was verified by DNA sequencing. The final vector was designated as **pUC57s-7FHL**. The plasmid was amplified via bacterial transformation in *E. Coli* Top10 competent cells.

2.1.7 Validation of Plasmid Vector Sequence

Before transcription/translation of the plasmid was performed, the DNA was re-sequenced to confirm proper identity. *E. Coli* Top10 competent cells containing the plasmid vector, sent initially from Creative Biolabs, were streaked onto LB agar plates containing ampicillin and grown overnight at 37°C. Single colonies were inoculated in 3-5 mL LB broth containing ampicillin and incubated for 16-18 hrs in a 37° C shaking incubator. The following day, plasmid was purified using a Qiagen Plasmid Mini Prep.

The appropriate primers were purchased and the DNA was amplified using PureTaq ready to go PCR beads from Fisher Scientific.

Restriction Digests were then performed to verify proper molecular weight of the vector. 5 μ L NeBuffer EcoRI + 0.5 μ L BSA + 33.5 μ L ddH₂O + 10 μ L DNA template (22.3 ng/ μ L) + 1 μ L EcoRI were added to a 1.5 mL vial to linearize the plasmid. 1 μ L EcoRI and 1 μ L Not I were then added to 5 μ L NeBuffer EcoRI + 0.5 μ L BSA + 32.5 μ L ddH₂O + 10 μ L DNA template (22.3 ng/ μ L) in order to confirm proper molecular weight of the insert. 5 μ L NeBuffer EcoRI + 0.5 μ L BSA, 32.5 μ L ddH₂O + 10 μ L PCR product + 1 μ L each of enzymes Eco RI and Not I were then added to a 1.5 mL vial. Each of the three samples were then mixed gently and placed at 37°C for 2 hours. Agarose gel analysis was performed and amplified DNA fragments resembling the insert were cut out from the gel and purified using a Qiaquick Gel Extraction Kit from Qiagen. Final product was sent out for sequencing.

2.1.8 Coupled Transcription/Translation of Purified Plasmid

For expression of the anti-NNK recombinant binding fragment, a TNT T7 Quick Coupled Transcription/Translation System from Promega was used. DNA was purified and then concentrated using a DNA Clean & ConcentratorTM-5 Kit from Zymo Research. Circular and linearized DNA templates were tested to determine which structure was most ideal for optimal protein expression. Final concentration of circular and linearized DNA used in the coupled transcription/translation reaction was 0.87 μ g and 0.45 μ g, respectively. 20 μ L TNT master mix, 0.5 μ L 1mM Methionine, 4 μ L DNA template (**circular plasmid**) and 0.5 μ L Canine Pancreatic Microsomal Membranes were added to

a 1.5 mL tube on ice and vortexed gently to properly mix. 20 μ L TNT master mix, 0.5 μ L 1 mM Methionine, 0.5 μ L T7 PCR Promoter enhancer, 4 μ L DNA template (**linearized plasmid**) and 0.45 μ L Canine Pancreatic Microsomal Membranes were added to a 1.5 mL tube on ice and mixed as above. The samples were then placed at 30° C for a total of 75 minutes per manufacturer's protocol.

2.1.9 Purification of Final Protein Product

After coupled transcription/translation of the linearized and circular plasmid was performed, the polyhistidine-tagged binding products were purified using the MagZTM Protein Purification System from Promega. 50 μ L circular and 50 μ L linearized plasmid from the coupled transcription/translation reaction were each applied to two empty 1.5 mL vials. 100 μ L each MagZ Binding/Wash Buffer was then added and vials were mixed by inverting slowly 5 times. Two 40 μ L aliquots of MagZ Binding Particles were then transferred to two empty 1.5 mL vials. Each tube was placed in a magnetic stand to allow for separation of binding particles from the supernatant. Next, each prepared protein solution from above was added to the vials containing the binding particles. The mixtures were carefully pipetted to re-suspend the particles in solution. The solutions were then incubated for 15 minutes at room temperature with gentle agitation to avoid settling of particles at bottom of tubes.

Supernatant from each vial was then removed by placing the vials in the magnetic stand in order to separate the beads from the mixture. 200 μ L MagZ Binding/Wash buffer was added to the particles and mixed by pipetting 5-6 times. Tubes were placed in the magnetic stand once again to facilitate supernatant removal. This wash step was

repeated 3 additional times. 100 μ L each of Elution Buffer was added to washed beads in both vials and mixed five times. Purified protein product was obtained by placing the vials in the magnetic stand and removing the supernatant.

2.1.10 Protein Concentration

Purified protein products were concentrated using a Protein Concentrate (Micro) Kit from Millipore (Temecula, Ca). 50 μ L of each sample were added to two vials containing 150 μ L each of UPPA-1 Buffer and incubated on ice for 15 minutes. 150 μ L UPPA-II buffer was then added, vials were vortexed and placed in a table top microcentrifuge at 10,000 rpm for 5 minutes. Supernatant was discarded and the pellets were each covered with 40 μ L UPC-Wash and centrifuged at 10,000 rpm for 5 minutes. Supernatant was collect and 25 μ L RNase free water was added to each of the protein pellets. Vials were centrifuged at 10,000 rpm for 30 seconds. 700 μ L pre-chilled Orgosol buffer and 3 μ L UPC-Seed was added to each vial, vortexed and then placed at -20° C for 30 minutes. During this period, vials were mixed intermittently for a total of 20 seconds at each time interval. Vials were then centrifuged once again at 10,000 rpm for a total of 5 minutes. The supernatant was collected and 15 μ L Precipitate Buffer I was added to each vial. After a 2 minute incubation on ice, 3 μ L Precipitate Buffer II was added to both vials. Samples were then incubated for 5 minutes on ice and centrifuged at 10,000 rpm for a total of 30 seconds. Clear supernatant containing the concentrated protein product was collected from each vial.

2.1.11 Re-Characterization of F(ab)-generating single chain antibody:

SDS-PAGE was performed to verify proper translation of the protein product. 20 μ L purified protein product + 3 μ L NuPAGE denaturing agent + 7.5 μ L SDS-PAGE reagent were added to a 10% polyacrylamide pre-packaged gel from NuPAGE. Proteins were resolved by running the reaction at 150 V for a total of 30 minutes. The gel was then stained using a Silver Staining Kit from Life Sciences in order to visualize the protein bands.

2.1.12 Western Blot Analysis

Protein bands were transferred to a PVDF membrane by running a Western Blot at 30 V for 60 minutes at 4 degrees Celsius. The membrane was incubated in 5% non-fat dry milk + TBS-T for one hour and then incubated with a 1:5,000 dilution of an anti-mouse IgG (Fab-specific) alkaline phosphatase conjugated antibody in blocking buffer, for a total of two hours. The membrane was then washed in TBS-T according to protocol and bands were developed by using a SIGMAFASTTM BCIP[®]/NBT tablet from Sigma-Aldrich.

2.1.13 Statistical Analysis

Statistical analysis was performed on data obtained from the F(ab) and 7F Competition ELISA. Using SAS 9.2 for Windows, the significance level α was set to 0.05% and a Mixed Procedure with a Diagonal Covariance Structure was performed.

Results

The mRNA from the 7F hybridoma V_H and V_L coding sequence was converted to cDNA, amplified, (**Figure 3.1.1**) sequenced and cloned into an expression vector with the FMDV 2A cleavage motif placed in-frame and between the two fragments (**Figure 3.1.2**). The resulting expression vector was used to transfect HEK293 cells to determine if a functional F(ab) was synthesized and secreted. Concentrated tissue culture supernatants were purified over an affinity column and the eluate analyzed by SDS-PAGE, which confirmed that the sequence was successfully translated, cleaved and secreted (**Figure 3.1.3**). Western Blots confirmed the presence of the heavy and light chain fragments at the predicted molecular weights, however a stronger band was observed for the 24 kD fragment (**Figure 3.1.4**). Competition studies using the anti-NNK binding fragment showed a concentration dependent inhibition of binding upon pre-incubation with free NNK, reaching 85% at the highest concentration tested (0.48 mM) (**Figure 3.1.5**).

Both a cell viability assay and proliferation assay were performed to determine the effects of NNK on transformed lung epithelial and adenocarcinoma cells. Results were inconclusive in that both A549 and NCI-H441 cells did not respond to varying concentrations of NNK (0.483 μ M-4,830 μ M) over an incubation period of 19-48 hrs.

In order to improve the binding affinity of the previously expressed F(ab), several adjustments were made to the initial plasmid constructed by Creative Biolabs. To the amplified V_L/V_H DNA sequence containing the FMDV 2A cleavage motif, a T7 Promoter, Kozak Sequence, ER cleavable signal sequence from Calreticulin, GSG Linker, His Tag and Synthetic Poly A tag plus suitable endonuclease enzyme sites were

added. All of these components were cloned into the expression vector pUC57 in order to yield the final product (**Figure 3.1.6**). The plasmid was sequenced (**Figure 3.1.7**), and then amplified for subsequent expression in a coupled transcription/translation cell-free system. The sequence of the plasmid was re-confirmed by performing Restriction Digests. Agarose Gel Analysis (**Figure 3.1.8**) confirmed that the plasmid amplified from *E-Coli* TOP10 transformed bacterial cells was in fact the correct Molecular Weight (4.2 Kb), and that digestion of the plasmid with enzymes NotI and EcoRI produced an insert of the anticipated size (1.6 Kb). SDS-PAGE analysis was inconclusive due to the presence of several protein bands of various molecular weights (**Figure 3.1.9**). These bands are most likely part of the rabbit reticulocyte lysate from the coupled transcription/translation reaction that were co-purified with the protein. In order to confirm that proper protein processing occurred, a Western Blot was performed using a 1:5000 dilution of an anti-mouse IgG (Fab-specific) antibody. Development of the PVDF membrane showed that protein bands were not present.

Figure 3.1.1: PCR amplification of the V_H and V_L Immunoglobulin chains of the 7F Mab.

mRNA from the 7F hybridoma was converted to cDNA and then amplified via PCR.

Results showed two individual bands of the appropriate molecular weights. LANE 1:

PCR amplification of the V_L with the κ primers; LANE 2: PCR amplification of the V_H

with the V_H back primers and CH1 for primers; M: molecular weight standard.

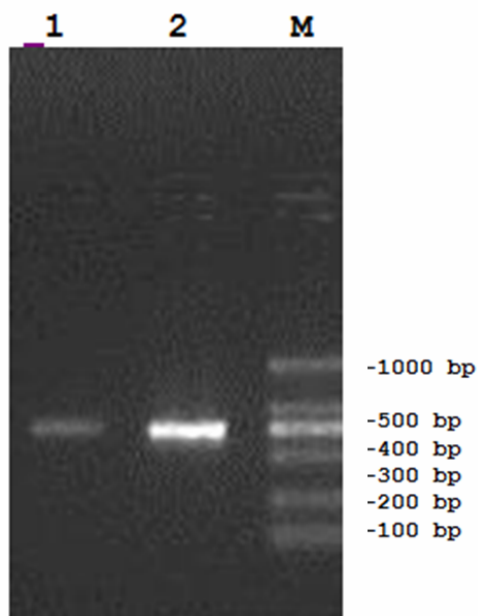


Figure 3.1.2: The schematic map of BSA-DP-pFab-H

The BSA-DP-pFab-H eukaryotic expression vector was expressed within HEK293 cells.

The DNA of the individual Ig chains, linked by the 2A sequence, was cloned into the vector via EcoRI/NotI.

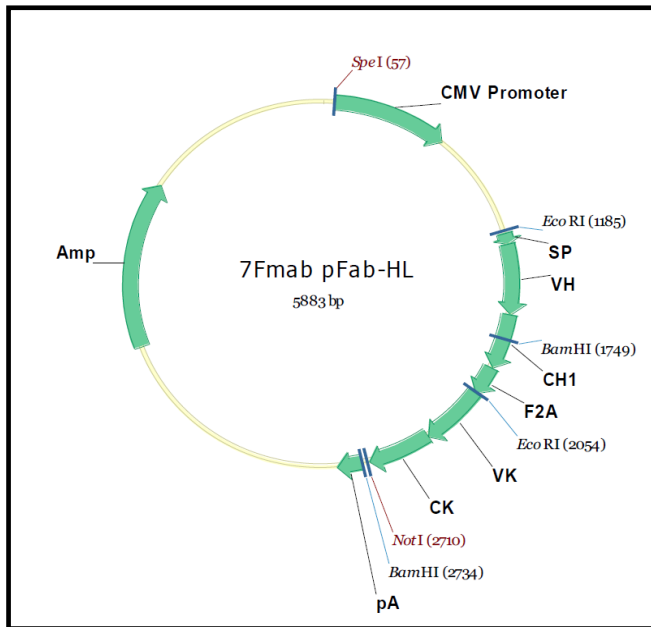
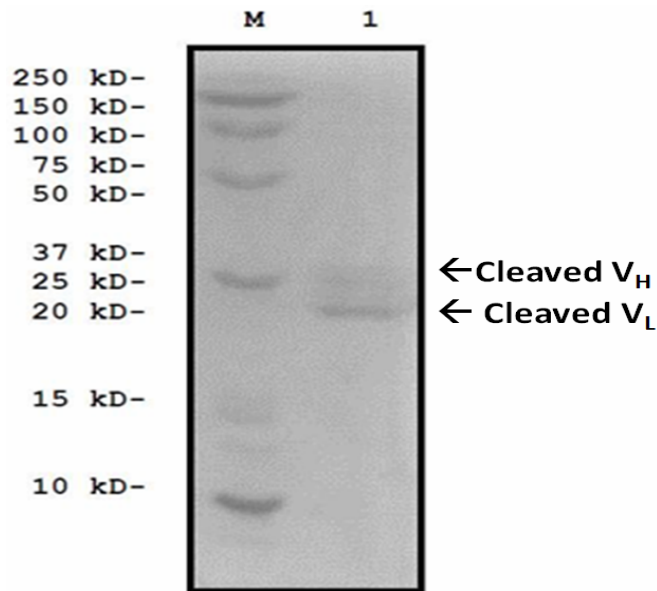


Figure 3.1.3: SDS-PAGE separation of purified Anti-NNK Binding Fragment

A non-denaturing SDS-PAGE revealed that expression of the F(ab) in HEK293 cells resulted in the successful cleavage of the fusion product into two individual Immunoglobulin chains at the anticipated molecular weights

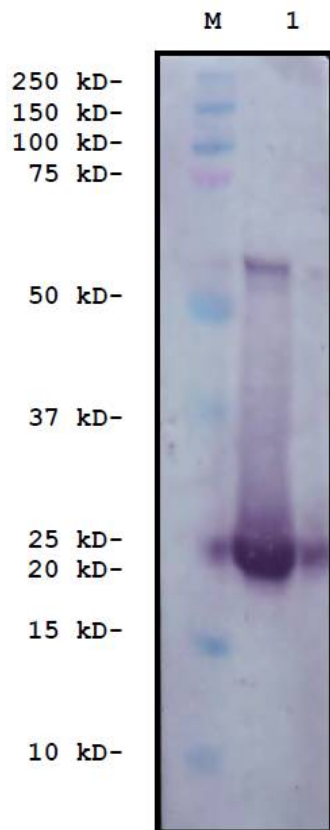


M: Molecular Weight standard

Lane 1: Cleaved VL and VH antibody chains

Figure 3.1.4: Western Blot

Western Blot analysis of the binding fragment expressed in HEK293 cells revealed the presence of two protein bands at the anticipated molecular weights. An anti-mouse IgG (Fab-specific) alk. phos. conjugated Ab was used at a 1:40,000 dilution for detection of the individual Immunoglobulin chains.



M: Molecular Weight Standard

Lane 1: VH and VL Immunoglobulin Chains at 1:40,000 dilution of primary Ab.

Figure 3.1.5: Competitive Inhibition of Anti-NNK Binding Fragment and 7F using free NNK

A 10 mg/mL stock solution of NNK was diluted to initial concentrations of 26 μ M, 88 μ M, 292 μ M, and 966 μ M. A 1:4 dilution of the F(ab) was added to each concentration of NNK to yield a final dilution of 1:8. Competition ELISA screening revealed that approximately 84% inhibition of the construct was seen at 483 μ M of NNK. At the same concentration of NNK, 85% inhibition of the monoclonal antibody 7F was evident.

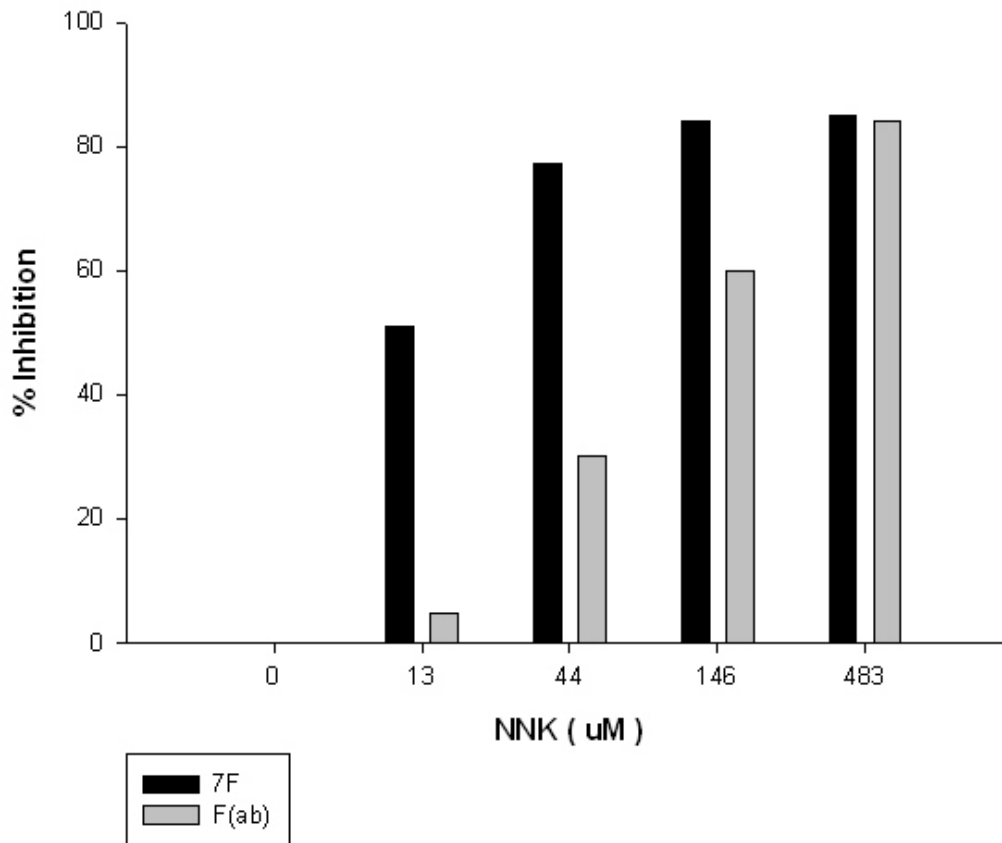


Figure 3.1.6: Final Plasmid Construct

7F VL-CL DNA was amplified from the original 7F Fab vector using the primers U7fvl/Dck and ligated into pUC57s via *Pst*I/*Mfe*I, yielding the vector designated as pUC57s-7FVLCL. 7F VH-CH1 DNA was amplified from the 7F Fab vector using the primers U7fvh/Dch1 and ligated into pUC57s-7FVLCL via *Sac*II/*Avr*II. The identity of the sequences were verified by DNA sequencing (**Figure 3.1.7**). The final vector was designated as pUC57s-7FHL.

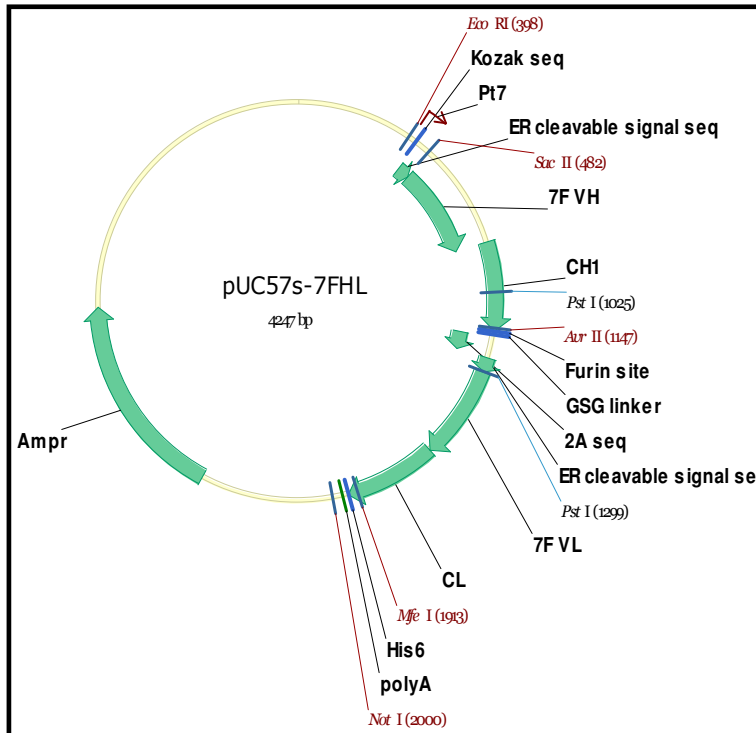


Figure 3.1.7: DNA sequence of Optimized Anti-NNK Binding Fragment

Purple = T7 Promoter
Underlined = Kozak Sequence
Yellow = ER cleavable signal sequence from Calreticulin
Light Green = Variable Heavy Chain
Light Blue = Constant Heavy Chain
Dark Yellow = Furin Site
Teal = GSG Linker
Grey = 2A sequence
Pink = Variable Light Chain
Red = Constant Light Chain
Green = His Tag
Dark Grey = Synthetic Poly A tag

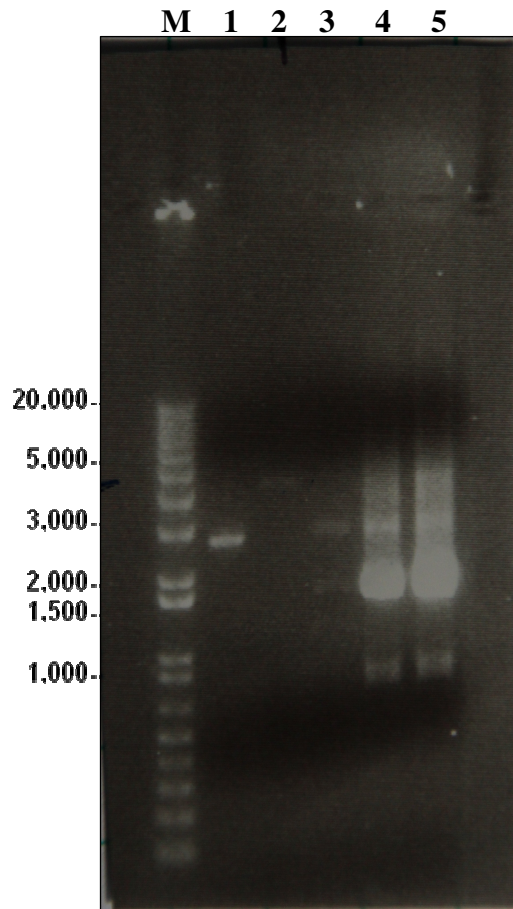
```

1  CGA ATT CGA CTA ATA CGA CTC ACT ATA GGG AGA GCC ACC ATG CTG CTC CCT GTG CCG CTG
61  CTG CTC GGC CTG CTC GGC CTG GCC GCG GCC GAG GTG AAG CTG GAT GAG ACT GGA GGA GGC
121 TTG GTG CAA CCT GGG AGG CCC ATG AAA CTC TCC TGT GTT GCC TCT GGA TTC ACT TTT AGT
181 GAC TAC TGG ATG AAC TGG GTC CGC CAG TCT CCA GAG AAA GGA CTG GAG TGG GTA GCA CAA
241 ATT AGA AAG AAA CCT TAT AAT TAT GAA ACA TAT TAT TCA GAT TCT GTG AAA GGC AGA TTC
301 ACC ATC TCA AGA GAT GAT TCC AAA AGT AGT GTC TAC CTG CAA ATG AAC AAC GTA AGA GCT
361 GAA GAC ATG GGT ATC TAT TAC TGT ACG GCC TAT GGT TAC GAC GAT TAC TAT ACT ATG GAC
421 TAC TGG GGT CAA GGA ACC TCA GTC ACC GTC TCC TCA GCC AAA ACG ACA CCC CCA TCT GTC
481 TAT CCA CTG GCC CCT GGA TCT GCT GCC CAA ACT AAC TCC ATG GTG ACC CTG GGA TGC CTG
541 GTC AAG GGC TAT TTC CCT GAG CCA GTG ACA GTG ACC TGG AAC TCT GGA TCC CTG TCC AGC
601 GGT GTG CAC ACC TTC CCA GCT GTC CTG CAG TCT GAC CTC TAC ACT CTG AGC AGC TCA GTG
661 ACT GTC CCC TCC AGC ACC TGG CCC AGC GAG ACC GTC ACC TGC AAC GTT GCC CAC CCG GCC
721 AGC AGC ACC ACG GTG GAC AAA AAA ATT GTG CCT AGG GAT TGT AGG AAG AGG CGA GGA TCC
781 GGA GCA CCT GTA AAG CAA ACA CTG AAC TTT GAC CTT CTC AAG TTG GCT GGA GAC GTT GAG
841 TCC AAT CCT GGG CCC ATG CTG CTC CCT GTG CCG CTG CTG CTC GGC CTG CTC GGC CTG GCT
901 GCA GCC GAC ATT GTG ATG ACC CAG TCT CAA AAA TTC ATG TCC ACA TCA GTA GGA GAC AGG
961 GTC AGC ATC ACC TGC AAG GCC AGT CAG AAT GTT CGT ACT GCT GTA GCC TGG TAT CAA CAG
1021 AAA CCA GGG CAG TCT CCT AAA GCA CTG ATT TAC TTG GCA TCC AAC CGG CAC ACT GGA GTC
1081 CCT GAT CGC TTC ACA GGC AGT GGA TCT GGG ACT GAT TTC ACT CTC ACC ATT AGC AAT GTG
1141 CAA TCT GAA GAC CTG GCA GAT TAT TTC TGT CTG CAA CAT TGG AAT TAT CCG TAC ACG TTC
1201 GGA GGG GGG ACC AAG CTG GAA ATA AAA CGG GCT GAT GCT GCA CCA ACT GTA TCC ATC TTC
1261 CCA CCA TCC AGT GAG CAG TTA ACA TCT GGA GGT GCC TCA GTC GTG TGC TTC TTG AAC AAC
1321 TTC TAC CCC AAA GAC ATC AAT GTC AAG TGG AAG ATT GAT GGC AGT GAA CGA CAA AAT GGC
1381 GTC CTG AAC AGT TGG ACT GAT CAG GAC AGC AAA GAC AGC ACC TAC AGC ATG AGC AGC
ACC
1441 CTC ACG TTG ACC AAG GAC GAG TAT GAA CGA CAT AAC AGC TAT ACC TGT GAG GCC ACT CAC
1501 AAG ACA TCA ACT TCA CCA ATT GTC AAG AGC TTC AAC AGG AAT GAG TGT CAC CAC
CAC CAC
1561 CAC CAC TAA AAA AAA AAA AAA AAA AAA AAA AAA AAA TGA GCG GCC GCT C
    
```

Figure 3.1.8: Gel Analysis of DNA from Reconstructed Plasmid

An agarose gel was run to confirm the identity of the pUC57s-7FHL expression vector.

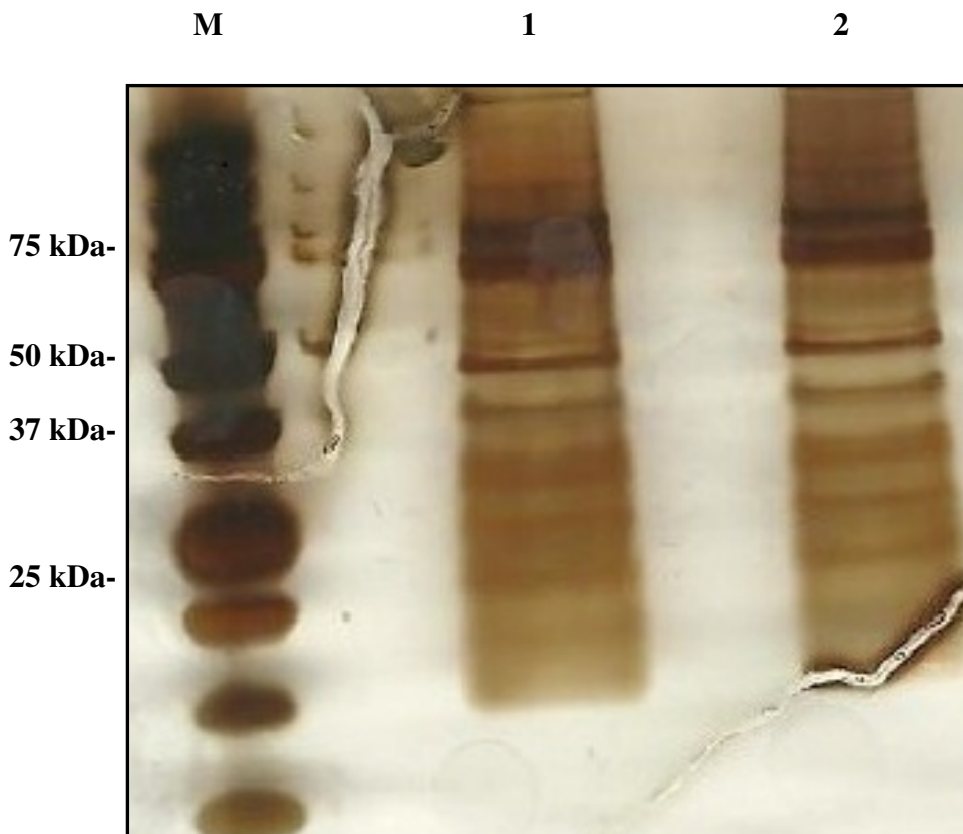
Restriction digests were performed using enzymes EcoRI and NotI. Gel analysis revealed that the vector contained the insert and at the appropriate molecular weight.



M: Molecular Weight Marker
Lane 1: Supercoiled Plasmid
Lane 2: Linearized Plasmid
Lane 3: Empty Plasmid + Insert
Lane 4: PCR Amplified Insert
Lane 5: PCR Amplified Insert

Figure 3.1.9: SDS-PAGE of Anti-NNK Binding Fragment

SDS-PAGE analysis was performed on the binding fragment expressed within the coupled transcription/translation system. Results portrayed the presence of several different protein bands at varying molecular weights, along with two bands at the anticipated molecular weights (25 kDa).



Lane 1= Linearized Sample
Lane 2= Supercoiled Sample
M= Molecular Weight Marker

Discussion

Immune-mediated sequestration of carcinogens and toxicants found in certain products is an attractive means to mitigate the harmful biological effects of these compounds. The following proposal demonstrates the feasibility of this approach when combating the carcinogen NNK, which is abundant in smokeless tobacco. Over the past few years, other studies have attempted to mitigate the acute toxicity effects of drugs such as cocaine, heroin, methamphetamine, colchicine, oleander and other related substances [26, 46, 47, 48]. This work builds upon these previous studies by attempting to create a high affinity recombinant anti-NNK binding site derived from a monoclonal antibody specific for NNK that was synthesized previously [49]. To increase the binding efficiency of the antibody fragment, an FMDV 2A peptide was cloned between the amplified V_H and V_L immunoglobulin chains of the monoclonal antibody. The incorporation of this self-cleaving peptide between multiple proteins within a single vector has been shown to significantly improve protein expression and is superior to the IRES approach in regards to the ratios of each translated protein translated [40, 41, 50].

Amplification and cloning of the V_H and V_L immunoglobulin chains derived from the 7F monoclonal antibody was successfully accomplished along with the incorporation of the 2A peptide linker. When the construct was expressed in HEK 293 cells, the formation of a recombinant binding fragment with a similar binding affinity to NNK as its parent hybridoma (7F) was seen. According to competition studies, there was about a one log loss in binding affinity.

In order to address the loss in binding affinity, the initial plasmid containing the insert was reconstructed. We hypothesized that the original signal peptide attached

upstream of the light chain may not have been removed upon cellular processing, thereby interfering with proper antibody folding. This would also account for the higher concentration of the variable light chain as seen in **Figure 3.1.4**. In the new construct, an ER cleavable signal sequence from calreticulin was placed upstream of both the heavy and light chains. A study by Felipe et al. (2004) showed that the incorporation of this signal sequence resulted in proper subcellular localization of two processing products [51]. Another improvement was the addition of a Gly-Ser-Gly linker between the upstream protein and the 2A peptide. Cleavage efficiency is significantly improved by incorporation of this linker due to increased flexibility and relaxation of unfavorable conformations [52,53,54, 55,56]. In order to express the protein in the TNT coupled Transcription/Translation Cell-Free system, a T7 promoter, Kozak sequence and synthetic poly A tag were also added to the plasmid vector. The incorporation of a poly-His tag to the C-terminus of the light chain facilitated purification of the translated protein product, which was accomplished by using the MagZ Protein Purification System from Promega. Standard nickel-based resins that are usually used for purification of polyhistidine-tagged proteins were not used in this instance due to the fact that hemoglobin from the rabbit reticulocyte lysate binds to the resin, resulting in its co-elution with the poly-histidine tagged protein.

Results from this experiment were inconclusive due to the fact that the Coupled Transcription/Translation system failed to produce an anti-NNK binding fragment. Since this cell-free system lacks microsomal membranes necessary for proper cellular processing and glycosylation of proteins, the addition of canine pancreatic microsomal membranes were necessary for protein expression. However, it has been shown that

addition of these membranes can sometimes inhibit the transcription/translation process by up to 50%. Since bacterial cells produced plasmid DNA at relatively small concentrations (20 ng/ μ L), it is also possible that not enough DNA was used for the coupled transcription/translation reaction, but it is more likely that proper subcellular processing of the protein failed to occur. Expression of the construct in HEK293 cells would overcome this obstacle since all necessary cellular components, including microsomal membranes, are available for proper protein production. Studies will be conducted in the future using this cellular system in order to properly express the anti-NNK binding fragment.

Exposure of transformed lung epithelial and adenocarcinoma cells (NCI-H441 and A549) to varying concentrations of NNK produced inconclusive results. Cells did not respond to NNK, even when incubated with very high concentrations (4,830 μ M). This finding contradicts several others showing NNK to be a strong tumor-promoter, even in minute quantities [57, 58, 6, 59]. One reason for this could be the aberrant mutation of $\alpha 7$ nicotinic acetylcholine receptors within the cells due to high cell passage number, which would render them unresponsive to NNK. As mentioned previously, NNK ligation with these receptors is essential to activation of primary transcription factors necessary for the promotion of cellular proliferation/differentiation. Another possible reason for this finding could be inactivation of the NNK itself. NNK is sensitive to light/ UV exposure and if pH conditions are not optimal, can break down rather easily. Future studies need to be conducted in order to test the validity/reliability of these results.

The current study provided proof of principal for the ability of a recombinant binding fragment derived from an anti-NNK monoclonal antibody to successfully

sequester the carcinogen. This work paves the way for potential tobacco harm reduction immunotherapeutics that may one day be marketed in order to provide a less hazardous product for long-term tobacco users.

References

1. Kalamida, D., K. Poulas, V. Avramopoulou, E. Fostieri, G. Lagoumintzis, K. Lazaridis, A. Sideri, M. Zouridakis, and S. J. Tzartos. 2007. Muscle and neuronal nicotinic acetylcholine receptors. Structure, function and pathogenicity. *The FEBS journal* 274:3799-3845.
2. WHO Study Group on Tobacco Product Regulation. Report on the scientific basis of tobacco product regulation: fourth report of a WHO study group. *World Health Organization technical report series*:1-83, 81 p following 83.
3. 1990. Western EEG Society, annual meeting. Santa Monica, CA, 15-16 February 1990. Abstracts. *Electroencephalography and clinical neurophysiology* 76:33P-36P.
4. Doll, R., R. Peto, J. Boreham, and I. Sutherland. 2004. Mortality in relation to smoking: 50 years' observations on male British doctors. *BMJ (Clinical research ed)* 328:1519.
5. Vardavas, C. I., A. B. Seidenberg, and G. N. Connolly. Regulating duty free sales and tobacco advertising in airports: a call for action. *Tobacco induced diseases* 9:7.
6. Akopyan, G., and B. Bonavida. 2006. Understanding tobacco smoke carcinogen NNK and lung tumorigenesis. *International journal of oncology* 29:745-752.
7. Talhout, R., T. Schulz, E. Florek, J. van Benthem, P. Wester, and A. Opperhuizen. Hazardous compounds in tobacco smoke. *International journal of environmental research and public health* 8:613-628.
8. Nilsson, R. The molecular basis for induction of human cancers by tobacco specific nitrosamines. *Regul Toxicol Pharmacol* 60:268-280.
9. 2007. Smokeless tobacco and some tobacco-specific N-nitrosamines. *IARC monographs on the evaluation of carcinogenic risks to humans / World Health Organization, International Agency for Research on Cancer* 89:1-592.
10. Peterson, L. A. Formation, repair, and genotoxic properties of bulky DNA adducts formed from tobacco-specific nitrosamines. *Journal of nucleic acids* 2010.
11. Jull, B. A., H. K. Plummer, 3rd, and H. M. Schuller. 2001. Nicotinic receptor-mediated activation by the tobacco-specific nitrosamine NNK of a Raf-1/MAP kinase pathway, resulting in phosphorylation of c-myc in human small cell lung carcinoma cells and pulmonary neuroendocrine cells. *Journal of cancer research and clinical oncology* 127:707-717.
12. Eisner, M. D., P. Jacob, 3rd, N. L. Benowitz, J. Balmes, and P. D. Blanc. 2009. Longer term exposure to secondhand smoke and health outcomes in COPD: impact of urine 4-(methylnitrosamino)-1-(3-pyridyl)-1-butanol. *Nicotine Tob Res* 11:945-953.
13. Yuan, J. M., W. P. Koh, S. E. Murphy, Y. Fan, R. Wang, S. G. Carmella, S. Han, K. Wickham, Y. T. Gao, M. C. Yu, and S. S. Hecht. 2009. Urinary levels of tobacco-specific nitrosamine metabolites in relation to lung cancer development in two prospective cohorts of cigarette smokers. *Cancer research* 69:2990-2995.
14. Hecht, S. S. 1999. DNA adduct formation from tobacco-specific N-nitrosamines. *Mutation research* 424:127-142.
15. De Buck, S. S., M. T. Schellenberger, C. Ensich, and C. P. Muller. Effects of antibodies induced by a conjugate vaccine on 4-(methylnitrosamino)-1-(3-

- pyridyl)-1-butanone absorptive transport, metabolism, and proliferation of human lung cells. *International journal of cancer* 127:513-520.
16. DeVore, N. M., and E. E. Scott. Nicotine and 4-(methylnitrosamino)-1-(3-pyridyl)-1-butanone binding and access channel in human cytochrome P450 2A6 and 2A13 enzymes. *The Journal of biological chemistry* 287:26576-26585.
 17. He, X. Y., J. Shen, X. Ding, A. Y. Lu, and J. Y. Hong. 2004. Identification of critical amino acid residues of human CYP2A13 for the metabolic activation of 4-(methylnitrosamino)-1-(3-pyridyl)-1-butanone, a tobacco-specific carcinogen. *Drug metabolism and disposition: the biological fate of chemicals* 32:1516-1521.
 18. Su, T., Z. Bao, Q. Y. Zhang, T. J. Smith, J. Y. Hong, and X. Ding. 2000. Human cytochrome P450 CYP2A13: predominant expression in the respiratory tract and its high efficiency metabolic activation of a tobacco-specific carcinogen, 4-(methylnitrosamino)-1-(3-pyridyl)-1-butanone. *Cancer research* 60:5074-5079.
 19. Hecht, S. S. 1999. Tobacco smoke carcinogens and lung cancer. *Journal of the National Cancer Institute* 91:1194-1210.
 20. Stepanov, I., P. Upadhyaya, S. G. Carmella, R. Feuer, J. Jensen, D. K. Hatsukami, and S. S. Hecht. 2008. Extensive metabolic activation of the tobacco-specific carcinogen 4-(methylnitrosamino)-1-(3-pyridyl)-1-butanone in smokers. *Cancer Epidemiol Biomarkers Prev* 17:1764-1773.
 21. Hecht, S. S. 1999. Chemoprevention of cancer by isothiocyanates, modifiers of carcinogen metabolism. *The Journal of nutrition* 129:768S-774S.
 22. Tsurutani, J., S. S. Castillo, J. Brognard, C. A. Granville, C. Zhang, J. J. Gills, J. Sayyah, and P. A. Dennis. 2005. Tobacco components stimulate Akt-dependent proliferation and NFkappaB-dependent survival in lung cancer cells. *Carcinogenesis* 26:1182-1195.
 23. Schuller, H. M. 2007. Nitrosamines as nicotinic receptor ligands. *Life sciences* 80:2274-2280.
 24. Rivenson, A., D. Hoffmann, B. Prokopczyk, S. Amin, and S. S. Hecht. 1988. Induction of lung and exocrine pancreas tumors in F344 rats by tobacco-specific and Areca-derived N-nitrosamines. *Cancer research* 48:6912-6917.
 25. Improgo, M. R., A. R. Tapper, and P. D. Gardner. Nicotinic acetylcholine receptor-mediated mechanisms in lung cancer. *Biochemical pharmacology* 82:1015-1021.
 26. Shen, J., L. Xu, T. K. Owonikoko, S. Y. Sun, F. R. Khuri, W. J. Curran, and X. Deng. NNK promotes migration and invasion of lung cancer cells through activation of c-Src/PKC α /FAK loop. *Cancer letters* 318:106-113.
 27. Gallego, X., S. Molas, A. Amador-Arjona, M. J. Marks, N. Robles, P. Murtra, L. Armengol, R. D. Fernandez-Montes, M. Gratacos, M. Pumarola, R. Cabrera, R. Maldonado, J. Sabria, X. Estivill, and M. Dierssen. Overexpression of the CHRNA5/A3/B4 genomic cluster in mice increases the sensitivity to nicotine and modifies its reinforcing effects. *Amino acids* 43:897-909.
 28. Meier, B. M., and D. Shelley. 2006. The fourth pillar of the Framework Convention on Tobacco Control: harm reduction and the international human right to health. *Public Health Rep* 121:494-500.

29. Kober, H., E. F. Kross, W. Mischel, C. L. Hart, and K. N. Ochsner. Regulation of craving by cognitive strategies in cigarette smokers. *Drug and alcohol dependence* 106:52-55.
30. Brennan, K. A., R. A. Lea, P. S. Fitzmaurice, and P. Truman. Nicotinic receptors and stages of nicotine dependence. *Journal of psychopharmacology (Oxford, England)* 24:793-808.
31. Coggins, C. R., M. Ballantyne, M. Curvall, and L. E. Rutqvist. The in vitro toxicology of Swedish snus. *Critical reviews in toxicology* 42:304-313.
32. Gartner, C. E., W. D. Hall, S. Chapman, and B. Freeman. 2007. Should the health community promote smokeless tobacco (snus) as a harm reduction measure? *PLoS medicine* 4:e185.
33. Rodu, B. The scientific foundation for tobacco harm reduction, 2006-2011. *Harm reduction journal* 8:19.
34. Cobb, C. O., M. F. Weaver, and T. Eissenberg. Evaluating the acute effects of oral, non-combustible potential reduced exposure products marketed to smokers. *Tobacco control* 19:367-373.
35. Rainey, C. L., P. A. Conder, and J. V. Goodpaster. Chemical characterization of dissolvable tobacco products promoted to reduce harm. *Journal of agricultural and food chemistry* 59:2745-2751.
36. Montoya, I. 2008. [Immunotherapies for drug addictions]. *Adicciones* 20:111-115.
37. Keizer, R. J., A. D. Huitema, J. H. Schellens, and J. H. Beijnen. Clinical pharmacokinetics of therapeutic monoclonal antibodies. *Clinical pharmacokinetics* 49:493-507.
38. Roiko, S. A., A. C. Harris, M. G. LeSage, D. E. Keyler, and P. R. Pentel. 2009. Passive immunization with a nicotine-specific monoclonal antibody decreases brain nicotine levels but does not precipitate withdrawal in nicotine-dependent rats. *Pharmacology, biochemistry, and behavior* 93:105-111.
39. Norman, A. B., M. R. Tabet, M. K. Norman, W. R. Buesing, A. J. Pesce, and W. J. Ball. 2007. A chimeric human/murine anticocaine monoclonal antibody inhibits the distribution of cocaine to the brain in mice. *The Journal of pharmacology and experimental therapeutics* 320:145-153.
40. Chan, H. Y., S. V. X. Xing, P. Kraus, S. P. Yap, P. Ng, S. L. Lim, and T. Lufkin. Comparison of IRES and F2A-based locus-specific multicistronic expression in stable mouse lines. *PloS one* 6:e28885.
41. Deng, W., D. Yang, B. Zhao, Z. Ouyang, J. Song, N. Fan, Z. Liu, Y. Zhao, Q. Wu, B. Nashun, J. Tang, Z. Wu, W. Gu, and L. Lai. Use of the 2A peptide for generation of multi-transgenic pigs through a single round of nuclear transfer. *PloS one* 6:e19986.
42. Hecht, S. S., S. G. Carmella, I. Stepanov, J. Jensen, A. Anderson, and D. K. Hatsukami. 2008. Metabolism of the tobacco-specific carcinogen 4-(methylnitrosamino)-1-(3-pyridyl)-1-butanone to its biomarker total NNAL in smokeless tobacco users. *Cancer Epidemiol Biomarkers Prev* 17:732-735.
43. Thomadaki, K., E. J. Helmerhorst, N. Tian, X. Sun, W. L. Siqueira, D. R. Walt, and F. G. Oppenheim. Whole-saliva proteolysis and its impact on salivary diagnostics. *Journal of dental research* 90:1325-1330.

44. Szymczak-Workman, A. L., K. M. Vignali, and D. A. Vignali. Design and construction of 2A peptide-linked multicistronic vectors. *Cold Spring Harbor protocols* 2012:199-204.
45. Laemmli, U. K. 1970. Cleavage of structural proteins during the assembly of the head of bacteriophage T4. *Nature* 227:680-685.
46. Treweek, J. B., and K. D. Janda. An antidote for acute cocaine toxicity. *Molecular pharmaceutics* 9:969-978.
47. Safadi, R., I. Levy, Y. Amitai, and Y. Caraco. 1995. Beneficial effect of digoxin-specific Fab antibody fragments in oleander intoxication. *Archives of internal medicine* 155:2121-2125.
48. Rouan, S. K., I. G. Otterness, A. C. Cunningham, H. E. Holden, and C. T. Rhodes. 1990. Reversal of colchicine-induced mitotic arrest in Chinese hamster cells with a colchicine-specific monoclonal antibody. *The American journal of pathology* 137:779-787.
49. Wanczyk, H., T. Barker, D. Rood, D. I. Zapata, A. R. Howell, S. K. Richardson, J. Zinckgraf, G. P. Marusov, M. A. Lynes, and L. K. Silbart. Cloning and Characterization of a Hybridoma Secreting a 4-(Methylnitrosamino)-1-(3-pyridyl)-1-butanone (NNK)-Specific Monoclonal Antibody and Recombinant F(ab). *Toxins* 5:568-589.
50. Mizuguchi, H., Z. Xu, A. Ishii-Watabe, E. Uchida, and T. Hayakawa. 2000. IRES-dependent second gene expression is significantly lower than cap-dependent first gene expression in a bicistronic vector. *Mol Ther* 1:376-382.
51. de Felipe, P., and M. D. Ryan. 2004. Targeting of proteins derived from self-processing polyproteins containing multiple signal sequences. *Traffic (Copenhagen, Denmark)* 5:616-626.
52. Lorens, J. B., D. M. Pearsall, S. E. Swift, B. Peelle, R. Armstrong, S. D. Demo, D. A. Ferrick, Y. Hitoshi, D. G. Payan, and D. Anderson. 2004. Stable, stoichiometric delivery of diverse protein functions. *Journal of biochemical and biophysical methods* 58:101-110.
53. Szymczak, A. L., C. J. Workman, Y. Wang, K. M. Vignali, S. Dilioglou, E. F. Vanin, and D. A. Vignali. 2004. Correction of multi-gene deficiency in vivo using a single 'self-cleaving' 2A peptide-based retroviral vector. *Nature biotechnology* 22:589-594.
54. Holst, J., A. L. Szymczak-Workman, K. M. Vignali, A. R. Burton, C. J. Workman, and D. A. Vignali. 2006. Generation of T-cell receptor retrogenic mice. *Nature protocols* 1:406-417.
55. Provost, E., J. Rhee, and S. D. Leach. 2007. Viral 2A peptides allow expression of multiple proteins from a single ORF in transgenic zebrafish embryos. *Genesis* 45:625-629.
56. Wargo, J. A., P. F. Robbins, Y. Li, Y. Zhao, M. El-Gamil, D. Caragacianu, Z. Zheng, J. A. Hong, S. Downey, D. S. Schrupp, S. A. Rosenberg, and R. A. Morgan. 2009. Recognition of NY-ESO-1+ tumor cells by engineered lymphocytes is enhanced by improved vector design and epigenetic modulation of tumor antigen expression. *Cancer Immunol Immunother* 58:383-394.
57. Hecht, S. S. 1998. Biochemistry, biology, and carcinogenicity of tobacco-specific N-nitrosamines. *Chemical research in toxicology* 11:559-603.

58. Zheng, H. C., and Y. Takano. NNK-Induced Lung Tumors: A Review of Animal Model. *Journal of oncology* 2011:635379.
59. Stabile, L. P., M. E. Rothstein, D. E. Cunningham, S. R. Land, S. Dacic, P. Keohavong, and J. M. Siegfried. Prevention of tobacco carcinogen-induced lung cancer in female mice using antiestrogens. *Carcinogenesis* 33:2181-2189.